

## Infection with *Mycobacterium ulcerans* Induces Persistent Inflammatory Responses in Mice

Martinha S. Oliveira,<sup>1</sup>† Alexandra G. Fraga,<sup>1</sup>† Egídio Torrado,<sup>1</sup> António G. Castro,<sup>1</sup> João P. Pereira,<sup>1</sup> Adhemar Longatto Filho,<sup>1,2</sup> Fernanda Milanezi,<sup>1,3</sup> Fernando C. Schmitt,<sup>1,3</sup> Wayne M. Meyers,<sup>4</sup> Françoise Portaels,<sup>5</sup> Manuel T. Silva,<sup>1,6</sup> and Jorge Pedrosa<sup>1\*</sup>

Life and Health Sciences Research Institute, School of Health Sciences (ICVS), University of Minho, Braga, Portugal<sup>1</sup>; Division of Pathology of Adolfo Lutz Institute, São Paulo, Brazil<sup>2</sup>; Institute of Molecular Pathology and Immunology, University of Porto, Porto, Portugal<sup>3</sup>; Armed Forces Institute of Pathology, Washington, D.C.<sup>4</sup>; Mycobacteriology Unit, Department of Microbiology, Institute of Tropical Medicine, Antwerp, Belgium<sup>5</sup>; and Institute for Molecular and Cell Biology, Porto, Portugal<sup>6</sup>

Received 7 January 2005/Returned for modification 11 February 2005/Accepted 31 May 2005

**Buruli ulcer (BU) is a devastating, necrotizing, tropical skin disease caused by infections with *Mycobacterium ulcerans*. In contrast to other mycobacterioses, BU has been associated with minimal or absent inflammation. However, here we show that in the mouse *M. ulcerans* induces persistent inflammatory responses with virulence-dependent patterns. Mycolactone-positive, cytotoxic strains are virulent for mice and multiply progressively, inducing both early and persistent acute inflammatory responses. The cytotoxicity of these strains leads to progressive destruction of the inflammatory infiltrates by postapoptotic secondary necrosis, generating necrotic acellular areas with extracellular bacilli released by the lysis of infected phagocytes. The necrotic areas, always surrounded by acute inflammatory infiltrates, expand through the progressive invasion of healthy tissues around the initial necrotic lesions by bacteria and by newly recruited acute inflammatory cells. Our observations show that the lack of inflammatory infiltrates in the extensive areas of necrosis seen in advanced infections results from the destruction of continuously produced inflammatory infiltrates and not from *M. ulcerans*-induced local or systemic immunosuppression. Whether this is the mechanism behind the predominance of minimal or absent inflammatory responses in BU biopsies remains to be elucidated.**

Pathogenic mycobacteria are intracellular parasites that are responsible for several clinically important infections in humans and animals. The most frequent mycobacterial infections in humans are caused by *Mycobacterium tuberculosis* and *M. leprae*. However, a unique group of mycobacterioses has been emerging and comprises infections caused by *M. marinum*, *M. hemophilum*, and *M. ulcerans* (12). These are slow-growing mycobacteria with some genetic relatedness (71) and common peculiar characteristics. These mycobacteria have optimal growth temperatures of 28 to 33°C and infect primarily the cooler parts of the body, mainly the skin. They have cytotoxic activity (17, 56, 57) and, as a consequence, produce necrotizing lesions (3, 7, 12, 72).

Buruli ulcer (BU), caused by *M. ulcerans*, has become the third most prevalent mycobacteriosis throughout the world, after tuberculosis and leprosy, with higher incidence in the tropical regions of western and central Africa (11, 74). BU is a devastating skin disease characterized by different clinical forms, including nonulcerative subcutaneous nodules, papules, edema, and plaques, that can eventually progress to ulcerative forms and often to extensive necrotic lesions (11, 74). Osteomyelitis has been described as a complication of *M. ulcerans* infection, particularly in some African regions (11, 39).

Genetic analyses showed that *M. marinum* and *M. ulcerans*

are very closely related to *M. tuberculosis* (71), a mycobacterium that also exhibits some cytotoxicity (14, 19, 37, 43), which contributes to the necrotic lesions seen in tuberculosis (43). Recently, genes in the extRD1 region have been implicated in the cytotoxic activity of *M. tuberculosis* and *M. marinum* (20). However, *M. ulcerans* is the most necrotizing of all mycobacteria due to the secretion of mycolactone, a unique polyketide lipid extoxin that has a potent necrotizing activity associated with extensive ulcerative lesions characteristic of the disease (22, 23). *M. ulcerans* mycolactone is considered the major pathogenicity factor in BU, and the genes that encode the biochemical machinery for its synthesis are carried on a 147-kb plasmid (69).

The inflammatory response to mycobacterial infections is characterized histopathologically by an early, acute, predominantly neutrophilic response (51, 59, 60, 62), which changes over time to a chronic, mononuclear, granulomatous pattern (10, 36). The histopathology of lesions produced by *M. tuberculosis*, *M. marinum*, or *M. hemophilum* shows these typical features of mycobacterial infections (3, 7, 12, 44, 72). It is therefore intriguing that *M. ulcerans*, despite being related to those mycobacteria, would produce a disease where minimal or absent inflammatory responses have been predominantly observed (6, 8, 9, 27, 30, 31). This view gained a consensus status and became a hallmark of the histopathology of *M. ulcerans* infection in human disease (1, 12, 15, 21–25, 35, 45, 48, 52, 64). Experimental *M. ulcerans* infections in mice, rats, guinea pigs, and nine-banded armadillos led to contradictory observations regarding induction of inflammatory responses. In some stud-

\* Corresponding author. Mailing address: Life and Health Sciences Research Institute, School of Health Sciences, University of Minho, 4710-057 Braga, Portugal. Phone: 351-253-604833. Fax: 351-253-604809. E-mail: jpedrosa@eceaude.uminho.pt.

† M.S.O. and A.G.F. contributed equally to this work.

ies, the occurrence of an inflammatory response was reported (38, 40, 57), but other studies showed minimal inflammation associated with *M. ulcerans* infection (22, 23, 75). Moreover, the dynamics of the infection process and host inflammatory response at different stages of infection with *M. ulcerans* are still poorly understood.

The present study was undertaken to evaluate the different stages of experimental *M. ulcerans* infection and associated cellular inflammatory responses. We examined the cytotoxicity and pathogenicity for mice of different clinical isolates of *M. ulcerans* by evaluating cell death of infected macrophages in vitro and lesions produced in a footpad mouse model of infection. We analyzed *M. ulcerans*-induced disease from the early stage of infection until later stages associated with ulceration, which allowed us to characterize the dynamics of the infectious process. We found that the mycolactone-producing strains have cytotoxic activity and proliferate in mouse footpads, inducing pathology, while the mycolactone-negative strain is noncytotoxic and nonvirulent. We also found that *M. ulcerans* consistently induces an early, acute neutrophilic inflammatory response that is independent of virulence, followed by prolonged cellular responses that differ according to the strain. With strains virulent for mice, the acute inflammatory infiltrate persisted throughout infection and consisted primarily of neutrophils and some macrophages and lymphocytes surrounding a central, expanding, necrotic acellular focus. In contrast, with the avirulent strain, the initial acute inflammatory response switched to a chronic inflammatory response with a persistent mononuclear infiltrate with few neutrophils, associated with granuloma-like structures and the absence of necrosis.

#### MATERIALS AND METHODS

**Mycobacterial strains and preparation of inocula.** The *M. ulcerans* strains used in this study were selected based on our preliminary studies that showed different degrees of virulence in mice. Moreover, the genetic and phenotypic characteristics of these strains, including production of mycolactone, had been previously described (4, 5, 45, 67). The strains are from the collection of the Institute of Tropical Medicine (ITM), Antwerp, Belgium, where they have been kept freeze-dried at  $-80^{\circ}\text{C}$  before being passaged to Löwenstein-Jensen (LJ) medium for the present study, as well as for recently published studies on their ability to produce mycolactone (45) and, in the case of strains 5114 and 98-912, on the structure of the plasmid that carries genes responsible for mycolactone synthesis (68). Strain 5114 was isolated from a case of ulcerative BU in Mexico in 1953 and was received in 1965 at the ITM. The ITM 5114 strain does not produce mycolactones (45) due to the loss of key genes involved in mycolactone synthesis (68). However, its growth characteristics on LJ and in 7H9 media as well as within cultured murine bone marrow-derived macrophages (BMDM) are comparable to those of the other two strains used (not shown). Strain 97-1116 was isolated from a plaque form of BU in Benin in 1997 and was found to produce mycolactones A/B (45). Strain 98-912 was isolated in China in 1997 from a case of ulcer; it produces mycolactones A/B (45), but it has recently been shown that the chemical structure of mycolactones A/B produced by this strain is slightly different from that of mycolactones A/B produced by an African strain (34). The clinical isolates were grown on LJ medium at  $32^{\circ}\text{C}$  for approximately 2 months. *M. ulcerans* was recovered from slants of LJ medium, diluted in phosphate-buffered saline (PBS) to a final concentration of 1 mg/ml, and vortexed vigorously using 2-mm glass beads. In all experiments, the number of acid-fast bacilli (AFB) in inocula was determined according to the method of Shepard and McRae (61), using Ziehl-Neelsen (ZN) staining (Merck, Darmstadt, Germany). The suspensions obtained according to this method revealed more than 90% viable cells (viability was assessed with the LIVE/DEAD BacLight kit from Molecular Probes, Leiden, The Netherlands) and minimal clump formation.

**Animals.** Eight-week-old female BALB/c mice were obtained from Charles River (Barcelona, Spain) and were housed under specific-pathogen-free conditions with food and water ad libitum.

**Culture of murine bone-marrow derived macrophages.** Macrophages were derived from the bone marrow as follows. Mice were euthanized with  $\text{CO}_2$  and femurs removed under aseptic conditions. Bones were flushed with 5 ml cold Hanks' balanced salt solution (HBSS) (Gibco, Paisley, United Kingdom). The resulting cell suspension was centrifuged at  $500 \times g$  and resuspended in Dulbecco's modified Eagle's medium (DMEM) (Gibco) supplemented with 10 mM HEPES (Sigma, St. Louis, MO), 1 mM sodium pyruvate (Gibco), 10 mM glutamine (Gibco), 10% heat-inactivated fetal bovine serum (Sigma), and 10% L929 cell conditioned medium (complete DMEM [cDMEM]). To remove fibroblasts or differentiated macrophages, cells were cultured for a period of 4 hours on cell culture dishes (Nunc, Naperville, IL) with cDMEM. Nonadherent cells were collected with warm HBSS, centrifuged at  $500 \times g$ , distributed in 24-well plates at a density of  $5 \times 10^5$  cells/well, and incubated at  $37^{\circ}\text{C}$  in a 5%  $\text{CO}_2$  atmosphere. A 0.1-ml amount of L929 cell conditioned medium was added 4 days after seeding, and medium was renewed on the seventh day. After 10 days in culture, cells were completely differentiated into macrophages. Twelve hours before infection, macrophages were incubated at  $32^{\circ}\text{C}$  in a 5%  $\text{CO}_2$  atmosphere and maintained until the end of the experimental infection as described elsewhere (50).

**Cytopathic effect of *M. ulcerans* strains on BMDM.** Bacterial suspensions were prepared as described above and further diluted in cDMEM before infecting macrophage monolayers. *M. ulcerans* suspensions (0.2 ml) were diluted in cDMEM and added to each well in order to obtain a multiplicity of infection (MOI) of 1:1 (bacteria/macrophage ratio). Cells were incubated for 4 h at  $32^{\circ}\text{C}$  in a 5%  $\text{CO}_2$  atmosphere and then washed four times with warm HBSS to remove noninternalized bacteria and reincubated in cDMEM for a maximum period of 8 days. To confirm the MOI, counting of AFB in infected macrophages was performed at the beginning of experimental infection as described previously (61). The cytopathic effect of different strains of *M. ulcerans* on macrophages was monitored for indicators of cytopathicity by using a phase-contrast microscope (22, 23) and by terminal deoxynucleotidyl transferase-mediated dUTP nick end labeling (TUNEL) staining by using an in situ cell death detection kit with fluorescein (Roche Diagnostics, Mannheim, Germany) according to the manufacturer's instructions. The coverslips were mounted in the antifading medium Vectashield (Vector, Peterborough, United Kingdom) with 4  $\mu\text{g}/\text{ml}$  of propidium iodide. TUNEL-positive nuclei stain yellow-green, and normal nuclei stain red. Cells were analyzed by fluorescence microscopy with a Zeiss Axioskop2 Plus microscope. Digital images were captured by using a AxioCam HRC camera (Zeiss, Hallbergmoos, Germany). As a control for cytotoxic activity of *M. ulcerans* strains, uninfected BMDM were analyzed at the same time intervals.

**Peritoneal model of infection.** Mice were infected in the peritoneal cavity with 0.1 ml of *M. ulcerans* suspensions containing 6  $\log_{10}$  *M. ulcerans* strain 5114, 97-1116, or 98-912 AFB; PBS was used as a control. At different time points after infection, four mice per group were sacrificed, and peritoneal cells were recovered by peritoneal lavage using 4 ml of PBS. Total leukocyte numbers were determined, and differential leukocyte counts were performed using cytopspin preparations fixed with 10% formol in ethanol and stained with Hemacolor (Merck).

**Footpad model of infection.** Mice were infected in the left hind footpad with 0.03 ml of *M. ulcerans* suspensions containing the numbers of AFB indicated for each experiment. The right hind footpad was used as a control. In other experiments, mice were infected in the left hind footpad with *M. ulcerans* 98-912 several days before inoculation of the contralateral footpad with 5  $\log_{10}$  AFB of the same strain. In all experiments, for ethical reasons, mice were sacrificed after ulceration of footpads.

**Assessment of footpad swelling and bacterial growth.** After infection, as an index of lesion development, footpad swelling of eight infected mice from each group was measured over time by using a caliper to measure the diameter of the frontal area of the footpad. *M. ulcerans* growth in footpad tissues of infected mice was evaluated. Briefly, tissue specimens were carefully minced on a petri dish after tendons and bones had been removed. The tissues were resuspended in 2 ml PBS containing 0.04% Tween 80 (Sigma) and vortexed vigorously with 2-mm glass beads to obtain homogenized suspensions. At different times postinfection, AFB counts were performed on samples from five footpads in each group by using the method of Shepard and McRae (61).

**Histological studies.** All excised tissues from control and infected footpads were fixed in 10% phosphate-buffered formalin. The whole paws were decalcified (Thermo Shandon TBD-1, Runcorn, United Kingdom) and embedded in paraffin. Longitudinal sections of the paws (4  $\mu\text{m}$ ) were processed for light microscopic studies after hematoxylin-eosin (HE) or ZN staining. For each sample, serial longitudinal sections of the entire paw were viewed under the microscope to ensure that representative areas of the lesions were analyzed. Several animals were studied for each time point as indicated in Table 1, and all histological

TABLE 1. Assessment of histopathological features after infection with different strains of *M. ulcerans*

Histopathological parameter	<i>M. ulcerans</i> strain	No. of positive cases/total studied cases on postinfection day:					
		2	7	15	24	43	60
Acute inflammation (predominant neutrophilic infiltrate)	98-912	5/5	2/6	6/6	6/6	— <sup>a</sup>	—
	97-1116	3/3	4/6	5/6	6/6	2/2	—
	5114	3/3	2/6	0/6	0/5	ND <sup>b</sup>	0/6
Chronic inflammation (predominant macrophagic-lymphocytic infiltrate)	98-912	0/5	4/6	0/6	0/6	—	—
	97-1116	0/3	1/6	1/6	0/6	0/2	—
	5114	0/3	4/6	6/6	5/5	ND	6/6
Presence of granuloma-like structures	98-912	0/5	0/6	0/6	0/6	—	—
	97-1116	0/3	0/6	0/6	0/6	0/2	—
	5114	0/3	0/6	6/6	5/5	ND	6/6
Leukocyte destruction (apoptosis/necrosis)	98-912	5/5	6/6	6/6	6/6	—	—
	97-1116	3/3	6/6	6/6	6/6	2/2	—
	5114	0/3	0/6	0/6	0/5	ND	0/6
Subcutaneous tissue necrosis	98-912	0/5	0/6	3/6	6/6	—	—
	97-1116	0/3	0/6	3/6	6/6	2/2	—
	5114	0/3	0/6	0/6	0/5	ND	0/6

<sup>a</sup> —, animals were sacrificed after emergence of ulceration.

<sup>b</sup> ND, not done.

observations were carried out blind. For TUNEL staining of paraffin sections, the In Situ Cell Death Detection Kit, AP (Roche Diagnostics), was used according to the manufacturer's instructions with the final contrast stain omitted. TUNEL-positive nuclei stain red; normal nuclei are unstained.

**Statistical analysis.** Statistical significance of values was determined using the Student *t* test.

## RESULTS

We first characterized the in vitro cytotoxicity as well as the in vivo pathology induced by three selected strains of *M. ulcerans*. Next, we analyzed the cellular inflammatory responses induced by these strains in the mouse peritoneal cavity and footpads.

***M. ulcerans* clinical isolates show different cytotoxicities against BMDM.** The genetic heterogeneity within *M. ulcerans* clinical isolates, which is caused by several factors, including instability and mutability of genes encoding the machinery for the synthesis of mycolactone, results in variable degrees of toxigenicity (68, 69). Cell lines treated with *M. ulcerans* culture filtrates, acetone-soluble lipids containing mycolactone, or purified mycolactone exhibit typical cytopathic changes (21–23, 45). However, the cytotoxicity of live *M. ulcerans* bacilli from different clinical isolates on infected macrophages has not been characterized. We first established an in vitro model of BMDM infection at 32°C in order to evaluate the cytotoxic activities of the different clinical isolates of *M. ulcerans* used in this study. Macrophage cultures were infected with *M. ulcerans* strain 5114, 97-1116, or 98-912 at a 1:1 MOI. No significant alterations were found in monolayers infected with strain 5114 compared to uninfected BMDM at 4 days (Fig. 1A and B) and at 8 days (data not shown) after infection. In contrast, strains 98-912 and 97-1116 are cytotoxic for macrophages, as assessed by cell rounding, shrinkage, and detachment of more than 90% of macrophages at 4 days (Fig. 1C and D). Positive TUNEL staining in a high proportion of macrophages (Fig. 1E) points to the apoptotic nature of that cytotoxicity.

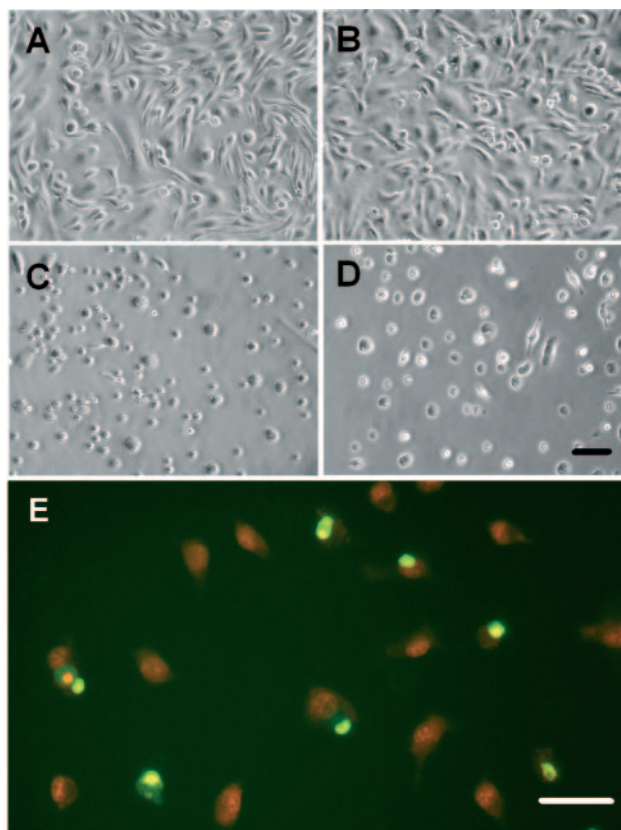


FIG. 1. Cytotoxicity of *M. ulcerans* clinical isolates to BMDM. BMDM were not infected (A) or were infected with *M. ulcerans* strain 5114 (B), 97-1116 (C), or 98-912 (D and E) at an MOI of 1:1. Macrophages were photographed 4 days after infection by phase-contrast microscopy (A to D) or with fluorescence microscopy for samples stained with TUNEL (E). Positive TUNEL staining (yellow-green fluorescent nuclei in E) points to the apoptotic nature of cell death induced by the cytotoxic strain 98-912. Bars, 50  $\mu$ m.

Since (i) the mycolactone-negative strain 5114 is noncytotoxic for macrophages, whereas the mycolactone-positive strains 98-912 and 97-1116 are cytotoxic, and (ii) this cytotoxicity is associated with cytopathic changes similar to those induced in fibroblast and macrophage cell lines by purified mycolactone (22, 23), we conclude that cytotoxicity of strains 98-912 and 97-1116 for BMDM correlates with mycolactone production.

**Cytotoxic *M. ulcerans* isolates are virulent for mice.** We measured over time the mean swelling of footpads infected with different strains of *M. ulcerans* as a macroscopic parameter for monitoring pathology. Significant differences were found in the mean swelling after inoculation of  $5 \log_{10}$  AFB of each *M. ulcerans* strain in the mouse footpad. Swelling was evident in mice infected with the cytotoxic *M. ulcerans* strain 98-912 during the second week of infection (Fig. 2A and B), and ulceration occurred by the end of the fourth week. Strain 97-1116 induced swelling of the footpad during the fourth week (Fig. 2A) and ulceration during the seventh week. In contrast, the noncytotoxic *M. ulcerans* strain 5114 was found not to induce significant swelling of the footpad up to 90 days of infection (Fig. 2A and B) or at 12 months postinoculation (data not shown). Infection of mice with  $2 \log_{10}$  AFB of *M. ulcerans* 98-912 showed that this strain still induced footpad swelling, albeit delayed, at concentrations 1,000-fold lower than the inoculum of *M. ulcerans* 5114 that did not induce measurable swelling (Fig. 2B).

To assess if the severity of lesions induced by *M. ulcerans* strains was associated with their capacity to proliferate in the host, we performed AFB counts in footpad homogenates. We found that *M. ulcerans* strains proliferated differently over the experimental period of infection. AFB counts following infection by *M. ulcerans* 98-912 increased significantly ( $P < 0.001$ ) from  $5.02 \log_{10}$  to  $7.90 \log_{10}$  between days 0 and 26 of infection (Fig. 2C). In mice infected with strain 97-1116, AFB counts increased approximately  $2 \log_{10}$  ( $P < 0.001$ ) from day 0 to day 39 postinfection (Fig. 2C). Conversely, *M. ulcerans* strain 5114 increased only from  $5.06 \log_{10}$  to  $5.69 \log_{10}$  ( $P < 0.01$ ) between days 0 and 16 postinfection and reached a plateau after 3 months (Fig. 2C) that remained stable after 12 months of infection (data not shown).

These results show that mycolactone-positive, cytotoxic strains of *M. ulcerans* are virulent for mice, while the mycolactone-negative, noncytotoxic strain is avirulent.

***M. ulcerans* induces an early acute inflammatory response in the peritoneal cavity.** Mycobacterioses, such as those caused by the *M. ulcerans*-related species *M. tuberculosis*, *M. marinum*, and *M. hemophilum*, have been consistently associated with acute and chronic recruitment of inflammatory cells to the site of infection (3, 7, 10, 36, 44, 51, 59, 60, 62, 72). However, reports on the histopathology of *M. ulcerans* infection are intriguing, since several authors describe minimal or absent cellular inflammation.

The mouse peritoneal model of infection has been used to characterize the inflammatory cellular response to mycobacterioses because it allows a precise qualitative and quantitative analysis of leukocyte populations (2, 51, 62). We used this model to evaluate quantitatively the early inflammatory response to *M. ulcerans* inoculation. After intraperitoneal infection with  $6 \log_{10}$  *M. ulcerans* 5114 AFB, 97-1116, or 98-912,

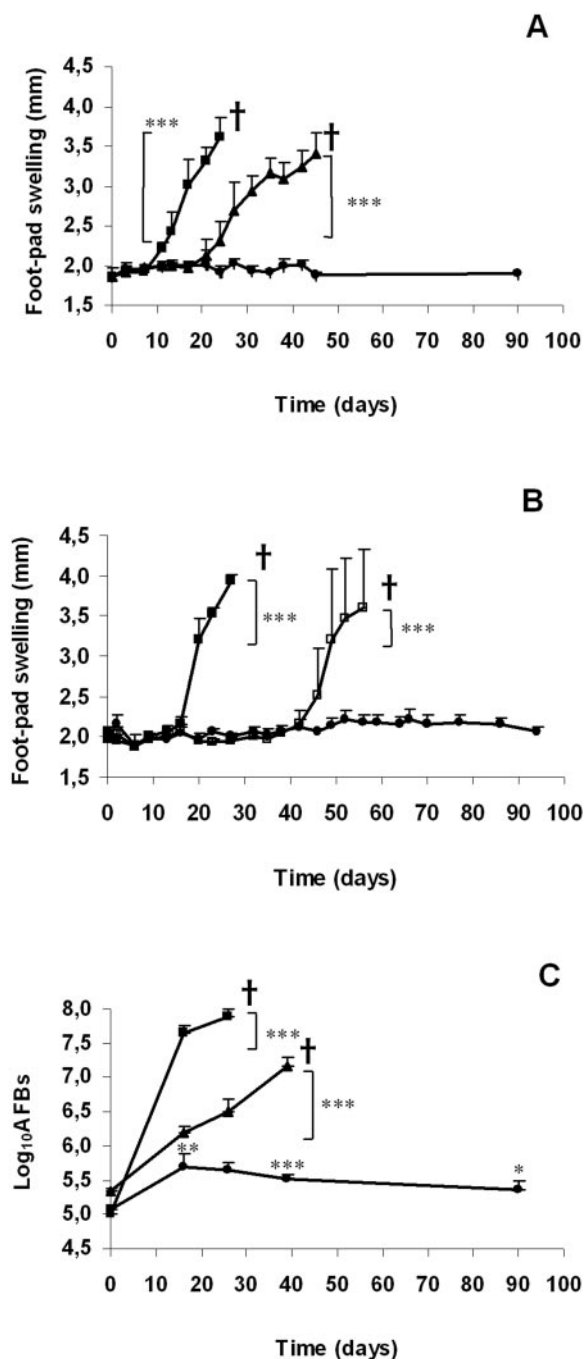


FIG. 2. Footpad swelling and proliferation of different strains of *M. ulcerans*. Panels A and C show swelling and AFB counts, respectively, of BALB/c mice footpads infected subcutaneously with  $5.0 \log_{10}$  AFB of *M. ulcerans* 98-912 (■),  $5.3 \log_{10}$  AFB of *M. ulcerans* 97-1116 (▲), or  $5.1 \log_{10}$  AFB of *M. ulcerans* 5114 (●). Panel B shows swelling of footpads infected with  $5.5 \log_{10}$  AFB (■) or  $2.5 \log_{10}$  AFB (□) of *M. ulcerans* 98-912 or  $5.5 \log_{10}$  AFB of *M. ulcerans* 5114 (●). Footpad swelling was measured in eight mice from each group. Significant differences in footpad swelling were calculated by comparing infected and noninfected mice. Significant differences in AFB counts were determined by comparing the bacterial loads of five footpads from each group with the respective initial inoculum. Calculations were performed using Student's *t* test (\*,  $P < 0.05$ ; \*\*,  $P < 0.01$ ; \*\*\*,  $P < 0.001$ ). Mice were sacrificed for ethical reasons after the emergence of ulceration (†). Results are from one representative of three independent experiments. Error bars indicate standard deviations.

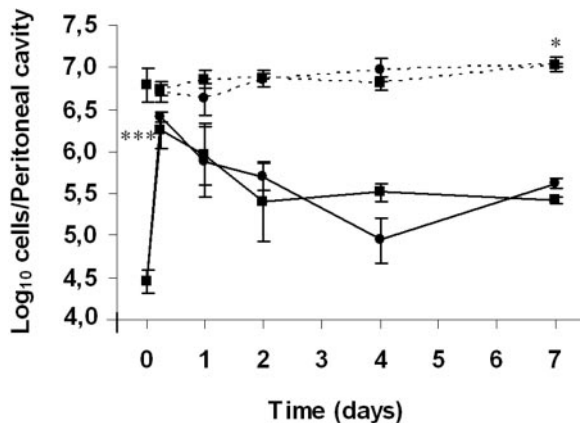


FIG. 3. Kinetics of recruitment of macrophages and neutrophils to the peritoneal cavity following infection with *M. ulcerans*. BALB/c mice were infected intraperitoneally with  $6.1 \log_{10}$  AFB of *M. ulcerans* 98-912 (■) or  $6.2 \log_{10}$  AFB of *M. ulcerans* 5114 (●). Peritoneal cells were recovered by peritoneal lavage, and the total number of leukocytes was determined. Counting of neutrophils (solid lines) and macrophages (dashed lines) was performed on Hemacolor-stained cytopins. \*,  $P < 0.05$ ; \*\*\*,  $P < 0.001$  (determined by Student's *t* test, comparing infected mice with mice inoculated with PBS). Results are from one representative experiment of two independent experiments. Error bars indicate standard deviations.

peritoneal exudates were collected at different time points. Total cell counts and differential leukocyte quantification were performed over a 2-week period. We found a significant recruitment of neutrophils and macrophages in mice infected with strains 5114 and 98-912 (Fig. 3) and 97-1116 (data not shown). The number of neutrophils increased more than 50-fold ( $P < 0.001$ ), peaked at 8 h postinfection, and declined afterwards but remained 10-fold above the initial value (Fig. 3). The number of monocytes/macrophages increased significantly 7 days after inoculation ( $P < 0.05$ ) (Fig. 3). No significant differences in other leukocyte populations were detected. Control mice injected intraperitoneally with PBS did not show a significant influx of neutrophils or macrophages (data not shown).

These results show for the first time that early recruitment of high numbers of neutrophils followed by an influx of monocytes/macrophages is a feature of *M. ulcerans* infection in the mouse, irrespective of the virulence of the isolates.

***M. ulcerans* induces extensive inflammatory responses in the mouse footpad.** Experimental infections of the mouse tail, ear, or footpad present several advantages over the peritoneal model for studying long-term infections by *M. ulcerans*, not only because of the nonpermissive temperature of the peritoneal cavity but also because it parallels the BU disease that affects the skin and subcutaneous tissue. Therefore, we used the footpad model of infection in order to characterize different phases of the inflammatory response to infection with *M. ulcerans*.

We performed a semiquantitative blind assessment of several histopathological parameters in sections of hind footpad tissue infected with  $5 \log_{10}$  AFB of *M. ulcerans* 98-912, 97-1116, or 5114, as summarized in Table 1. We found that the three strains induced an early and intense acute inflammatory cellular response in infected footpads. Within the first hours

after inoculation, we observed acute inflammatory responses showing a predominance of neutrophils with scattered macrophages and lymphocytes (Fig. 4A, B, G, H, M, and N), and with numerous bacilli within neutrophils and macrophages (not shown), as previously described (16).

However, the progression of histological features associated with pathology during experimental infection is largely dependent on the virulence of the *M. ulcerans* strain. Leukocyte destruction became apparent in the initial acute inflammatory infiltrate as early as 24 h after inoculation of the mouse-virulent strains 98-912 and 97-1116, as described in more detail in the next section. This cell death process leads to the production of necrotic, acellular foci (Fig. 4E, F, K, and L) that continuously expand during infection. The centrifugal advancement of cell destruction leaves behind cell debris and freed extracellular bacilli that accumulate in the necrotic areas (Fig. 5A, D, F, and G). This is accompanied by progressive invasion of healthy tissues by acute inflammatory infiltrates around the areas where previous infection led to necrotic destruction of acute infiltrates (Fig. 4E and K and 5A and D). The initiation of a switch from acute infiltrates, predominantly neutrophilic, to infiltrates with a majority of mononuclear cells, characteristic of chronic inflammation, as seen in some mice at day 7 postinfection, is not fully accomplished (Table 1). Instead, in the boundary between the expanding necrotic, acellular areas and the surrounding normal tissue, a band of acute cellular infiltrate is permanently present (Fig. 4C to F and I and L and 5A and D). The central necrotic area shows a high number of extracellular bacilli (Fig. 4F and L and 5A, D, F, and G), but the surrounding infiltrate of neutrophils, macrophages, and lymphocytes shows intracellular bacilli, mainly in macrophages (Fig. 5B, C, and E). As a result of the progression of this process, by the second or third week of infection with strain 98-912 or 97-1116, respectively, histological features of dermal edema are prominent, coinciding with the onset of footpad swelling (Fig. 2A), and necrosis extends to components of the subcutaneous tissue including fat. In advanced lesions, the necrotic areas with abundant free bacilli and absence of cells reach considerable extension (Fig. 5F and G). Eventually, multifocal microulcers emerge and result in extensive ulceration of the epidermis; only at this advanced stage did we observe secondary infection (data not shown).

Mice infected with  $2 \log_{10}$  AFB of *M. ulcerans* 98-912 (Fig. 2B) developed pathology with histological features similar to those observed in mice infected with  $5 \log_{10}$  AFB of the same strain, albeit with delayed kinetics (data not shown). We also assessed whether *M. ulcerans*-infected mice could mount acute inflammatory responses to reinfection with *M. ulcerans*. For this purpose, the left footpads were infected with  $5 \log_{10}$  AFB of *M. ulcerans* 98-912 until all mice showed progressive infection. After 35 days of infection, the contralateral footpads were injected with a similar dose of *M. ulcerans* 98-912 and analyzed after 10, 24, and 48 h. We found, in all experiments, that early, acute inflammatory responses are initiated in a manner similar to that described above for mice infected only once (data not shown).

In contrast, mice infected with the avirulent strain 5114 showed absence of necrotic alterations during the whole experimental period (Fig. 4M to R). The initial neutrophilic inflammatory process (Fig. 4M and N) was gradually replaced

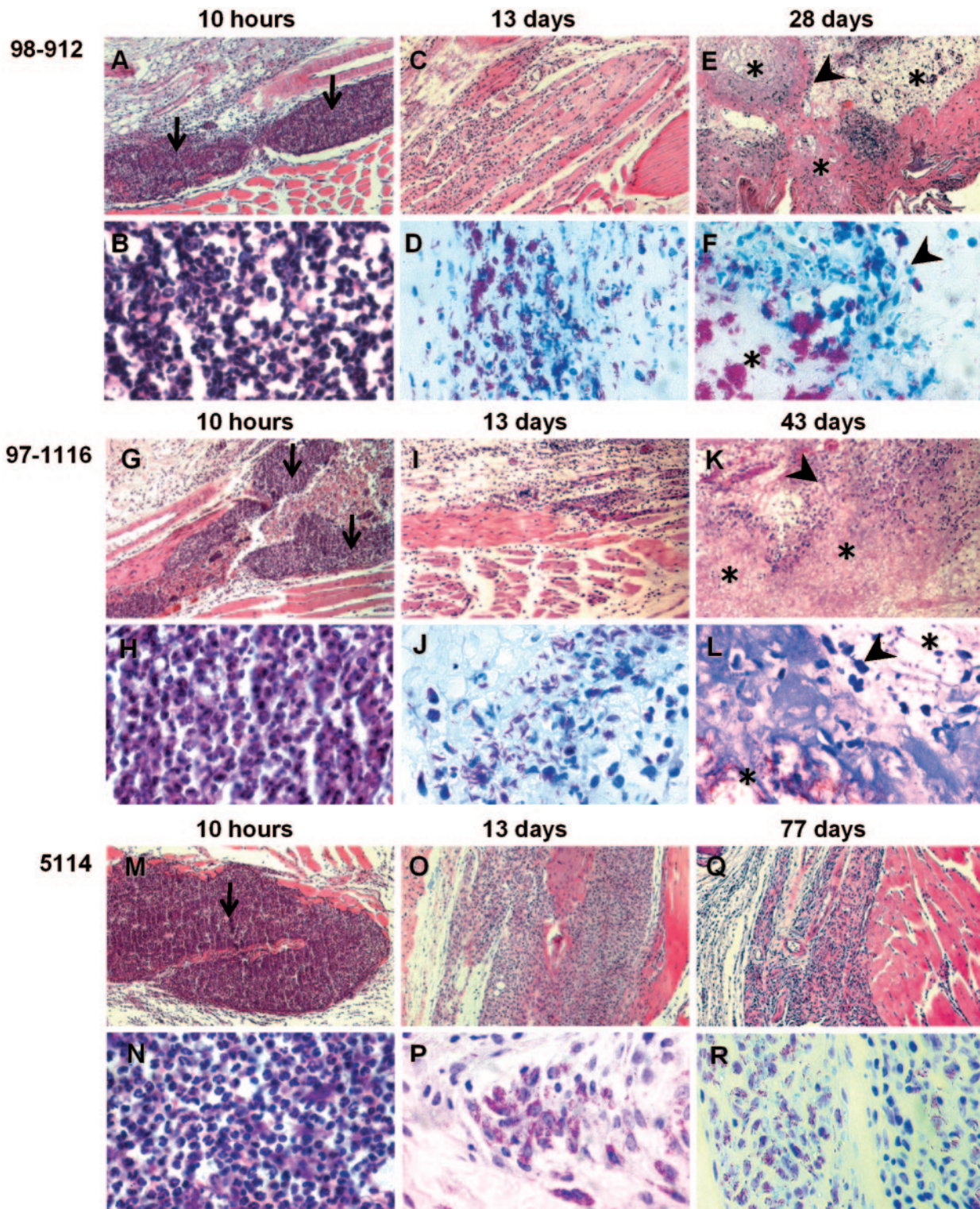


FIG. 4. Histological sections of footpads of mice infected with *M. ulcerans*. BALB/c mice were infected with  $5.9 \log_{10}$  AFB of *M. ulcerans* 98-912 (A to F),  $5.5 \log_{10}$  AFB of *M. ulcerans* 97-1116 (G to L), or  $5.8 \log_{10}$  AFB of *M. ulcerans* 5114 (M to R). Footpads were collected at the indicated times postinfection, and tissue sections were stained with HE (A, B, C, E, G, H, I, K, M, N, O, and Q) or ZN (D, F, J, L, P, and R). Magnifications,  $\times 60$  (A, C, E, G, I, K, M, O, and Q) and  $\times 350$  (B, D, F, H, J, L, N, P, and R). Panels A, B, G, H, M, and N show an acute inflammatory response with predominance of neutrophils (arrows) early after infection by all strains of *M. ulcerans*. Panels C to F and I to L depict advanced stages of infection with *M. ulcerans* 98-912 or 97-1116, respectively, and show necrosis of the central focus of infection (E, F, K, and L, asterisks) and high numbers of extracellular bacteria (F and L), surrounded by a band of acute cellular infiltrate (E and K, arrowheads). In contrast, advanced stages of infection with *M. ulcerans* 5114 show predominantly mononuclear infiltrates with intracellular bacilli, epithelioid transformation (O to R), and granuloma-like organization (P). Results are from one representative experiment of two independent experiments.

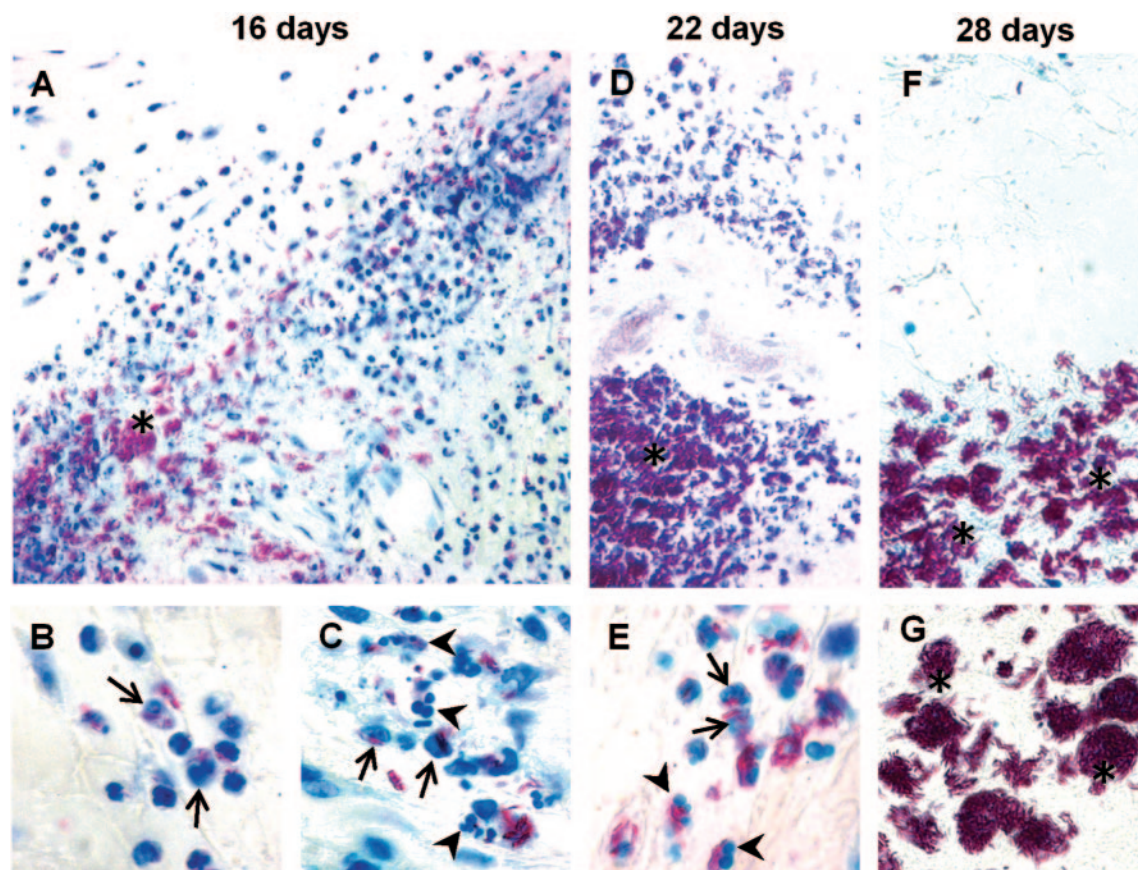


FIG. 5. Histological sections of lesions at late stages of infection with a mouse-virulent *M. ulcerans* strain. Footpads of mice infected with  $5.9 \log_{10}$  AFB of *M. ulcerans* 98-912 were analyzed at 16 (A, B, and C), 22 (D and E), or 28 (F and G) days postinfection. Tissue sections were stained with ZN. Magnifications,  $\times 250$  (A, D, and F) and  $\times 680$  (B, C, E, and G). Panels A, D, and F show acellular necrotic areas that are extensive in advanced infections (F), associated with extracellular bacilli (asterisks), surrounded by a band of acute inflammatory cellular infiltrate (A and D); the acute infiltrate at the periphery of the necrotic area in F is outside the micrograph. Higher magnifications of the acute infiltrates in A and D show intracellular bacilli (arrows in panels B, C, and E) and leukocyte death with pyknosis and karyorrhexis (arrowheads in panels C and E).

at the second week after infection by a predominantly lymphocytic and macrophagic infiltrate (Fig. 4O to R) with epithelioid transformation, in the presence of a small number of neutrophils (Table 1). During the remaining time of experimental infection, a predominance of lymphocytes, macrophages, and giant cells was maintained, together with granuloma-like organization (Fig. 4P) and some neutrophils. We found intracellular bacilli throughout the whole experimental period of infection (Fig. 4P and R).

These observations confirmed the occurrence of an acute cellular inflammation in the subcutaneous tissue, with the typical early and extensive recruitment of neutrophils in response to the infection with different strains of *M. ulcerans*, irrespective of their virulence for mice. In addition, our data showed that areas of cellular inflammation persist until the later stages of infection, with a cellular pattern varying according to the virulence of the strain.

**Mouse-virulent strains of *M. ulcerans* induce postapoptotic secondary necrosis.** It has been shown that *M. ulcerans* and its exotoxin mycolactone induce cell destruction in guinea pig skin (22, 23), in fibroblast and macrophage cell lines (22, 23), and in BMDM (Fig. 1E) by a cell death process with characteristics of apoptosis. We found that the destructive process affecting cell

populations of acute inflammatory infiltrates in footpads infected with mouse-virulent *M. ulcerans* strains, described in the previous section, shows morphological features of apoptotic cell death, namely pyknosis and karyorrhexis (77) (Fig. 6A, C, and E) and TUNEL positivity of pyknotic and fragmented nuclei (Fig. 6C). The dying cells were present in areas with bacilli (Fig. 6D and F) or close to bacilli. However, we did not find phagocytosis by macrophages of the cells undergoing apoptosis. This observation, together with the presence of abundant cell debris mixed with cells undergoing apoptosis (Fig. 6B and E), indicates that the cell death process proceeds to secondary necrosis (77). Therefore, massive postapoptotic cell lysis in the areas of acute inflammatory infiltrate rich in or close to bacilli is the process responsible for the production of expanding necrotic, acellular areas.

## DISCUSSION

In humans, infections by *M. ulcerans* have been extensively characterized by minimal or absent inflammation (1, 6, 8, 9, 12, 15, 21–26, 30, 31, 35, 45, 48, 52, 64), which contrasts with what is known to occur with other mycobacterioses (3, 7, 10, 12, 36, 44, 51, 59, 60, 62, 72). On the other hand, the experimental

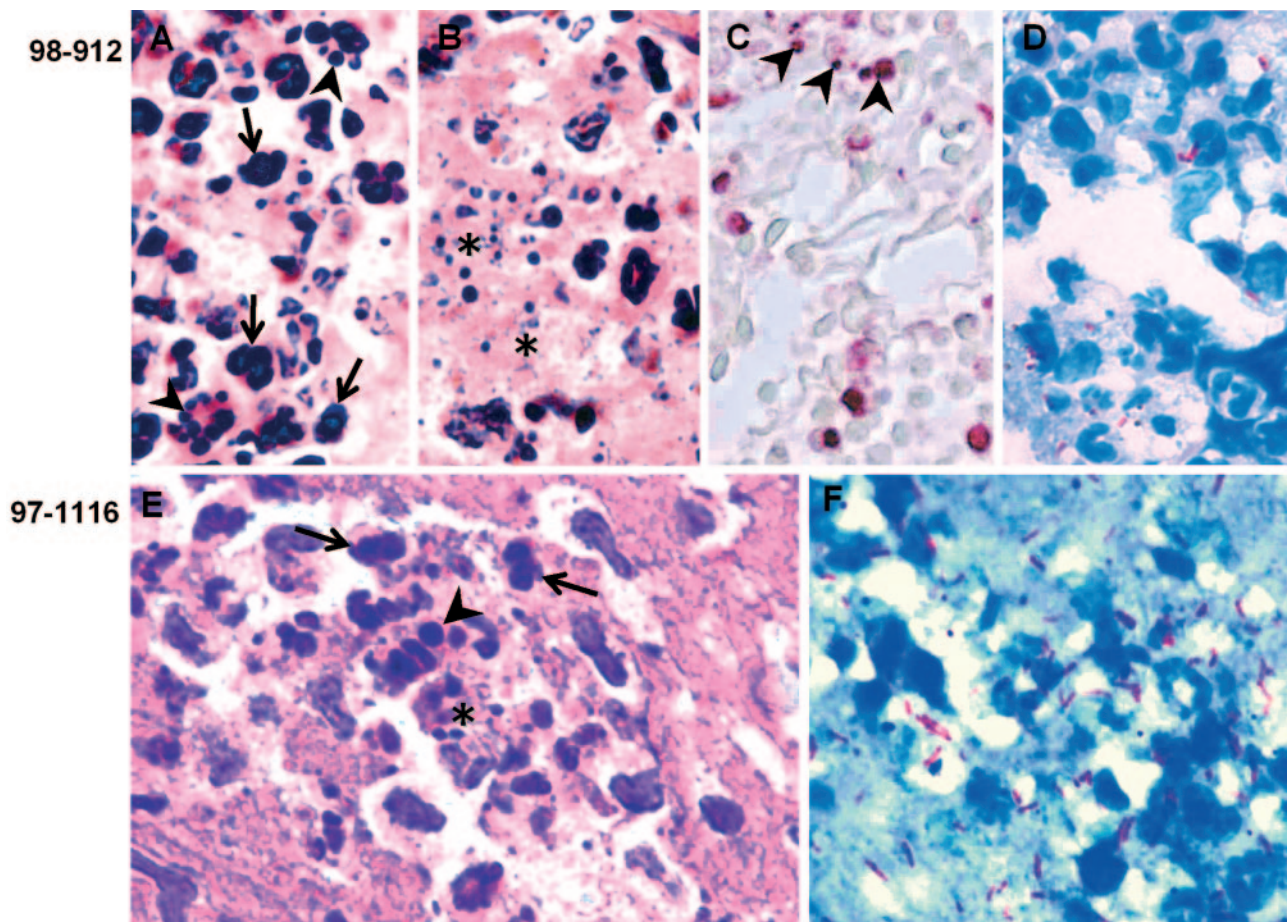


FIG. 6. Histological sections of inflammatory infiltrates at early stages of infection with mouse-virulent *M. ulcerans* strains. Mouse footpads were inoculated with  $5.9 \log_{10}$  AFB of *M. ulcerans* 98-912 (A to D) or  $5.5 \log_{10}$  AFB of *M. ulcerans* 97-1116 (E and F) for 24 h (A to D) or 48 h (E and F). Serial tissue sections (A to D and E and F) were stained with HE (A, B, and E), TUNEL (C), or ZN (D and F). Magnifications,  $\times 750$  (C),  $\times 1,000$  (A, B, and E), and  $\times 1,250$  (D and F). These panels show leukocyte cell death colocalized with bacilli in the acute inflammatory infiltrate (D and F), with evidence of pyknosis (A and E, arrows), karyorrhexis (A, C, and E, arrowheads), and cellular debris (B and E, asterisks). TUNEL staining (red nuclei and nuclear fragments in C) points to the apoptotic nature of cell death.

models of infection by *M. ulcerans* led to contradictory results regarding inflammatory responses (22, 23, 38, 40, 57, 75). Therefore, comprehensive analyses of infection with different *M. ulcerans* clinical isolates were carried out in mice to understand the dynamics of inflammatory responses in an animal model largely used in the study of experimental infections, including mycobacteriosis (18, 47), and to compare the histopathological features of *M. ulcerans* infections in mice and humans. Here we show that *M. ulcerans* induces relevant, virulence-dependent inflammatory responses in the mouse. The mycolactone-negative, noncytotoxic strain does not produce progressive infection and induces an initial acute neutrophilic response that switches to a chronic mononuclear infiltrate associated with granuloma-like structures, in the absence of necrosis. The two mycolactone-positive, cytotoxic strains multiply progressively and induce an acute inflammatory response that is permanently present during the infectious process, although at spatially restricted areas surrounding a central necrotic, acellular focus that expands with the progress of the disease.

The dynamics of the cellular response against infections has been thoroughly described and is characterized by an early,

acute inflammation enriched in neutrophils, followed by recruitment of monocytes that complement the activity of neutrophils (58). This biphasic phagocytic response is characteristic of infections caused by pathogenic *Mycobacterium* species related to *M. ulcerans*, such as *M. tuberculosis* and *M. marinum* (3, 7, 36, 44, 51, 60, 62, 72), and was now found to occur also in the mouse model of *M. ulcerans* infection. We show that the *M. ulcerans*-induced initial inflammatory response is indistinguishable in mice infected with mycolactone-positive or -negative strains. This suggests that production of mycolactone by *M. ulcerans* does not inhibit recruitment of phagocytes. The comprehensive semiquantitative and blind histological analyses carried out in the present study showed that in mice infected with mouse-virulent *M. ulcerans* strains, acute leukocyte responses are present, not only in the beginning of infection but also throughout the entire murine infectious process until ulceration of the footpad. Cell lysis in the acute inflammatory infiltrate became evident early in the infection with these virulent strains and led to the production of expanding necrotic areas. A band of acute cellular infiltrate is constantly present at the periphery of these necrotic areas and is colonized with



intraphagocytic bacilli. In contrast, abundant extracellular bacilli are seen in the expanding necrotic areas devoid of inflammatory cells. These necrotic areas reach considerable extension in advanced lesions and are similar to the necrotic areas predominantly described in human biopsies. Whether the above mechanism is behind the predominance of minimal or absent inflammatory responses in BU biopsies remains to be elucidated.

A switch from the initial acute, predominantly neutrophilic response to a chronic, predominantly mononuclear response, associated with epithelioid and giant cells and formation of granulomas, is typical of mycobacterial infections when a cellular-mediated immunity (CMI) is mounted (36, 44). As shown, in progressive murine infection by virulent *M. ulcerans*, such a switch is not fully completed. This observation correlates with the finding that progressive infection of the skin, disseminated disease, and osteomyelitis in BU patients were associated with an absence of granulomas in the infected areas (33, 49, 66). Conversely, with the noncytotoxic strain 5114, which is not virulent for mice and does not cause leukocyte death and necrosis of the subcutaneous tissue at any stage of infection, the acute neutrophilic profile of the cellular infiltrate gradually switches to a predominance of mononuclear cells and formation of granuloma-like structures. Not surprisingly, this type of chronic response was observed in BU patients during the healing phase of disease (30, 31, 40, 49, 66, 74).

We were able to observe early and continued acute, predominantly neutrophilic responses to mouse-virulent *M. ulcerans* strains because the small size of the diseased area allowed the systematic observation of the entire lesion and surrounding healthy tissues even in advanced infections when the areas of necrosis are extensive.

Our interpretation is that the areas of minimal or absent cellular inflammation seen in infected foci in mouse footpads with advanced infections with virulent *M. ulcerans* strains are due not to the lack of recruitment of inflammatory cells but rather to the destruction of preexistent inflammatory infiltrates. It is likely that such a destruction is due to the potent cytotoxic activity of mycolactone, because lysing leukocytes that colocalize with intracellular bacilli, or are in proximity to extracellular bacilli, show morphological features compatible to those described for the cytopathic activity of mycolactone (22, 23) and do not occur with the mycolactone-negative strain. Whether the observed difference in virulence for mice between strains 98-912 and 97-1116 are related to possible differences in the molecular structures of their mycolactones (34) requires further investigations. The diffusibility of this exotoxin and the high potency and wide cellular spectrum of its cytotoxicity explain the difference between the peculiar histopathology of *M. ulcerans* infections and that observed during infections with other related mycobacterium species, such as *M. marinum*, *M. hemophilum*, and *M. tuberculosis*.

Consequently, our observations show that the lack of significant inflammatory infiltrates in the necrotic areas of advanced murine infections is not the result of an inhibition of recruitment of inflammatory cells due to local immunosuppressive activity of *M. ulcerans* (48, 52). The finding that recruitment of inflammatory cells also occurs in the contralateral footpads of mice with well-established progressive infections indicates that systemic immunosuppression (24, 25) is not responsible for the

absence of inflammatory infiltrates, as well. Additionally, our observations also argue against the suggestion that the minimal or absent inflammation would be due to a lack of recruitment of inflammatory cells, because the cell destruction occurring in *M. ulcerans*-infected foci is due to apoptotic cell death (23). Indeed, this death process is usually associated with absence of inflammatory responses, because apoptotic cells are typically phagocytosed before lysis (41). However, we observed that apoptotic cells present in the infectious foci are not eliminated by phagocytosis so that this cell death proceeds to lytic secondary necrosis (77). This appears to be due to the overwhelming extension of mycolactone-induced apoptosis that affects all cell types of the infiltrate, including macrophages, the professional scavengers responsible for eliminating apoptotic cells (41). It is well known that postapoptotic secondary necrosis is a potent stimulus of inflammation, mainly when it affects high numbers of neutrophils (28), leukocytes rich in highly cytotoxic molecules (32).

In summary, we present here a time-lapse study of murine infection with *M. ulcerans* that dissects the dynamic characteristics of the host-parasite relationship at the site of active infection. Our interpretation of the progression of infection with virulent *M. ulcerans* in mouse footpads is as follows (Fig. 7). (i) Leukocyte death in the initial acute cellular infiltrate is induced early after infection, resulting in necrotic, acellular areas. Lysis of infected phagocytes results in the shedding of bacilli that accumulate in the necrotic areas. (ii) The phlogistic activity at the site of active infection and of cellular destruction at the periphery of the necrotic areas recruits new inflammatory infiltrates. (iii) In turn, the newly infected phagocytes are lysed, and the cycle is repeated. The number of bacilli increases and leads to the progressive invasion of adjacent healthy tissue by bacilli and inflammatory infiltrates and expansion of the necrotic area in a centrifugal manner. Consequently, from the beginning of infection with virulent *M. ulcerans* in mice, acute cellular inflammation is consistently present, although in advanced lesions it is spatially restricted to a narrow zone at the periphery of extensive necrotic, acellular areas.

The occurrence of a persistent influx of neutrophils, monocytes/macrophages and lymphocytes to the sites of active infection, as shown in the present study, provides the continuous availability of immune cells for interaction with *M. ulcerans*, as is the case with other mycobacterioses. The occurrence of this interaction in murine *M. ulcerans* infections is in accordance with the observation that *M. ulcerans*-infected mice exhibit CMI to both *M. bovis* BCG and its purified Ag85 complex (70). As discussed above, in human *M. ulcerans* infections the occurrence of similar interactions has not been considered. In fact, BU has been described as a disease with a histopathological pattern characterized by minimal or absent inflammatory responses and by the presence of abundant extracellular bacilli in extensive necrotic, acellular areas (6, 8, 9, 27, 30, 31). Although it is evident that such a histopathological pattern is a diagnostic hallmark of BU, it may not reflect all the aspects of the host-parasite interaction at the active infection foci. Indeed, there are several lines of evidence implicating CMI and delayed-type hypersensitivity responses in human *M. ulcerans* infections, favoring the possible existence of a phase of intracellularity of the pathogen, as follows. Studies with humans show that resistance to *M. ulcerans* is associated with the Th1

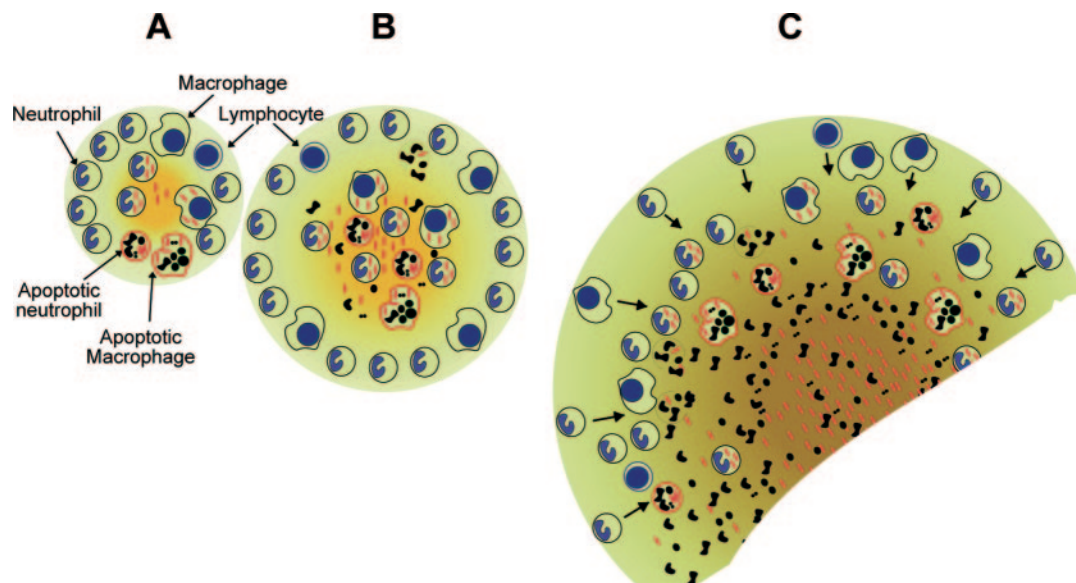


FIG. 7. Schematic representation of the progression of BU. Panel A shows *M. ulcerans* (red bacilli) being phagocytosed in the initial stage of infection by neutrophils and macrophages that are present in the early acute inflammatory infiltrate. Panel B represents a more advanced infection stage characterized by the onset of cell destruction, showing predominant neutrophilic cell infiltrate, apoptotic neutrophils and macrophages, and cell debris resulting from postapoptotic secondary necrosis. Panel C highlights an advanced stage of BU with extensive acellular areas with numerous extracellular bacilli, tissue damage represented by accumulation of cellular fragments, continued predominance of neutrophils, and low number of macrophages and lymphocytes. This stage is reminiscent of what has been observed in biopsies of advanced BU. The orange-yellow gradient represents the production and spreading of *M. ulcerans* exotoxin.

type of response (24, 25, 26, 55, 76), while a shift to a Th2 phenotype is related to susceptibility (26), and point to a protective effect of BCG vaccination (46, 53, 54, 63, 66, 73). Additionally, as BU disease progresses to healing, granuloma formation occurs (30, 31, 35, 40, 49, 66, 74), and the burulin skin test (65) tends to change from negative to positive (13, 42). In contrast, disseminated disease and osteomyelitis were reported to be associated with defects in granuloma formation (33, 39).

Taking into account that (i) CMI and delayed-type hypersensitivity occur not only in murine *M. ulcerans* infections but also in human BU; (ii) in the murine model, as shown in this study, extensive necrotic areas with extracellular bacilli that resemble the classical BU histopathology coexist, in advanced phases, with inflammatory infiltrates and intracellular bacilli; (iii) there are reports describing inflammatory infiltrates with intracellular bacilli in other animal models of infection; and (iv) a recent publication (29) reports the occurrence of infiltrates with neutrophils and mononuclear cells in 92% of 78 biopsies of confirmed BU, studies directed to the evaluation of the interactions between phagocytes and *M. ulcerans* in human infections are justified.

#### ACKNOWLEDGMENTS

This work was supported by a grant from the Health Services of Fundação Calouste Gulbenkian and by Fundação para a Ciência e a Tecnologia Praxis Fellowships SFRH/BI/9762/2003, SFRH/BI/11841/2003, and SFRH/BD/9757/2003 to M. S. Oliveira, A. G. Fraga, and E. Torrado, respectively.

We thank P. L. Small and R. E. Thomas for helpful discussions and critical reading of the manuscript, Ana do Vale and Carolina Costa-Ramos for help with TUNEL staining, and Goreti Pinto for laboratory assistance.

#### REFERENCES

- Abalos, F. M., J. Aguiar, Sr., A. Guendon, F. Portaels, and W. M. Meyers. 2000. *Mycobacterium ulcerans* infection (Buruli ulcer): a case report of the disseminated nonulcerative form. *Ann. Diagn. Pathol.* **4**:386–390.
- Appelberg, R., J. M. Pedrosa, and M. T. Silva. 1991. Host and bacterial factors control the *Mycobacterium avium*-induced chronic peritoneal granulocytosis in mice. *Clin. Exp. Immunol.* **83**:231–236.
- Busam, K. J., T. E. Kiehn, S. P. Salob, and P. L. Myskowski. 1999. Histologic reactions to cutaneous infections by *Mycobacterium haemophilum*. *Am. J. Surg. Pathol.* **23**:1379–1385.
- Chemlal, K., K. De Ridder, P. A. Fonteyne, W. M. Meyers, J. Swings, and F. Portaels. 2001. The use of IS2404 restriction fragment length polymorphisms suggests the diversity of *Mycobacterium ulcerans* from different geographical areas. *Am. J. Trop. Med. Hyg.* **64**:270–273.
- Chemlal, K., G. Huys, P. A. Fonteyne, V. Vincent, A. G. Lopez, L. Rigouts, J. Swings, W. M. Meyers, and F. Portaels. 2001. Evaluation of PCR-restriction profile analysis and IS2404 restriction fragment length polymorphism and amplified fragment length polymorphism fingerprinting for identification and typing of *Mycobacterium ulcerans* and *M. marinum*. *J. Clin. Microbiol.* **39**:3272–3278.
- Clancey, J. K., O. G. Dodge, H. F. Lunn, and M. L. Oduori. 1961. Mycobacterial skin ulcers in Uganda. *Lancet* **278**:951–954.
- Clark, R. B., H. Spector, D. M. Friedman, K. J. Oldrati, C. L. Young, and S. C. Nelson. 1990. Osteomyelitis and synovitis produced by *Mycobacterium marinum* in a fisherman. *J. Clin. Microbiol.* **28**:2570–2572.
- Connor, D. H., and H. F. Lunn. 1965. *Mycobacterium ulcerans* infection (with comments on pathogenesis). *Int. J. Lepr.* **33**:698–709.
- Connor, D. H., and H. F. Lunn. 1966. Buruli ulceration. A clinicopathologic study of 38 Ugandans with *Mycobacterium ulcerans* ulceration. *Arch. Pathol.* **81**:183–199.
- Dannenbergh, A. M., Jr. 1994. Pathogenesis of pulmonary tuberculosis: an interplay of time-damaging and macrophage-activating immune responses. Dual mechanisms that control bacillary multiplication, p. 459–483. In B. R. Bloom (ed.), *Tuberculosis: pathogenesis, protection and control*. American Society for Microbiology, Washington, D.C.
- Debacker, M., J. Aguiar, C. Steunou, C. Zinsou, W. M. Meyers, J. T. Scott, M. Dramaix, and F. Portaels. 2004. *Mycobacterium ulcerans* disease: role of age and gender in incidence and morbidity. *Trop. Med. Int. Health* **9**:1297–1304.
- Dobos, K. M., F. D. Quinn, D. A. Ashford, C. R. Horsburgh, and C. H. King. 1999. Emergence of a unique group of necrotizing mycobacterial diseases. *Emerg. Infect. Dis.* **5**:367–378.

13. Dobos, K. M., E. A. Spotts, B. J. Marston, C. R. Horsburgh, Jr., and C. H. King. 2000. Serologic response to culture filtrate antigens of *Mycobacterium ulcerans* during Buruli ulcer disease. *Emerg. Infect. Dis.* **6**:158–164.
14. Dobos, K. M., E. A. Spotts, F. D. Quinn, and C. H. King. 2000. Necrosis of lung epithelial cells during infection with *Mycobacterium tuberculosis* is preceded by cell permeation. *Infect. Immun.* **68**:6300–6310.
15. Evans, M. R., H. S. Thangaraj, and M. H. Wansbrough-Jones. 2000. Buruli ulcer. *Curr. Opin. Infect. Dis.* **13**:109–112.
16. Fenner, F. 1956. The pathogenic behavior of *Mycobacterium ulcerans* and *Mycobacterium balnei* in the mouse and the developing chick embryo. *Am. Rev. Tuberc.* **73**:650–673.
17. Fischer, L. J., F. D. Quinn, E. H. White, and C. H. King. 1996. Intracellular growth and cytotoxicity of *Mycobacterium haemophilum* in a human epithelial cell line (Hec-1-B). *Infect. Immun.* **64**:269–276.
18. Flynn, J. L., and J. Chan. 2001. Immunology of tuberculosis. *Annu. Rev. Immunol.* **19**:93–129.
19. Gadea, I., J. Zapardiel, P. Ruiz, M. I. Gegundez, J. Esteban, and F. Soriano. 1993. Cytotoxic effect mimicking virus culture due to *Mycobacterium tuberculosis*. *J. Clin. Microbiol.* **31**:2517–2518.
20. Gao, L. Y., S. Guo, B. McLaughlin, H. Morisaki, J. N. Engel, and E. J. Brown. 2004. A mycobacterial virulence gene cluster extending RD1 is required for cytolysis, bacterial spreading and ESAT-6 secretion. *Mol. Microbiol.* **53**:1677–1693.
21. George, K. M., L. P. Barker, D. M. Welty, and P. L. Small. 1998. Partial purification and characterization of biological effects of a lipid toxin produced by *Mycobacterium ulcerans*. *Infect. Immun.* **66**:587–593.
22. George, K. M., D. Chatterjee, G. Gunawardana, D. Welty, J. Hayman, R. Lee, and P. L. Small. 1999. Mycolactone: a polyketide toxin from *Mycobacterium ulcerans* required for virulence. *Science* **283**:854–857.
23. George, K. M., L. Pascopella, D. M. Welty, and P. L. Small. 2000. A *Mycobacterium ulcerans* toxin, mycolactone, causes apoptosis in guinea pig ulcers and tissue culture cells. *Infect. Immun.* **68**:877–883.
24. Gooding, T. M., P. D. Johnson, D. E. Campbell, J. A. Hayman, E. L. Hartland, A. S. Kemp, and R. M. Robins-Browne. 2001. Immune response to infection with *Mycobacterium ulcerans*. *Infect. Immun.* **69**:1704–1707.
25. Gooding, T. M., P. D. Johnson, M. Smith, A. S. Kemp, and R. M. Robins-Browne. 2002. Cytokine profiles of patients infected with *Mycobacterium ulcerans* and unaffected household contacts. *Infect. Immun.* **70**:5562–5567.
26. Gooding, T. M., A. S. Kemp, R. M. Robins-Browne, M. Smith, and P. D. Johnson. 2003. Acquired T-helper 1 lymphocyte anergy following infection with *Mycobacterium ulcerans*. *Clin. Infect. Dis.* **36**:1076–1077.
27. Goutzamanis, J. J., and G. L. Gilbert. 1995. *Mycobacterium ulcerans* infection in Australian children: report of eight cases and review. *Clin. Infect. Dis.* **21**:1186–1192.
28. Gregory, C. D., and A. Devitt. 2004. The macrophage and the apoptotic cell: an innate immune interaction viewed simplistically? *Immunology* **113**:1–14.
29. Guarner, J., J. Bartlett, E. A. Whitney, P. L. Raghunathan, Y. Stienstra, K. Asamo, S. Etuafu, E. Klutse, E. Quarshie, T. S. Van Der Werf, W. T. Van Der Graaf, C. H. King, and D. A. Ashford. 2003. Histopathologic features of *Mycobacterium ulcerans* infection. *Emerg. Infect. Dis.* **9**:651–656.
30. Hayman, J. 1993. Out of Africa: observations on the histopathology of *Mycobacterium ulcerans* infection. *J. Clin. Pathol.* **46**:5–9.
31. Hayman, J., and A. McQueen. 1985. The pathology of *Mycobacterium ulcerans* infection. *Pathology* **17**:594–600.
32. Henson, P. M., and R. B. Johnson, Jr. 1987. Tissue injury in inflammation. Oxidants, proteinases, and cationic proteins. *J. Clin. Investig.* **79**:669–674.
33. Hofer, M., B. Hirschel, P. Kirschner, M. Beghetti, A. Kaelin, C. A. Siegrist, S. Suter, A. Teske, and E. C. Bottger. 1993. Disseminated osteomyelitis from *Mycobacterium ulcerans* after a snakebite. *N. Engl. J. Med.* **328**:1007–1009.
34. Hong, H., J. B. Spencer, J. L. Porter, P. F. Leadlay, and T. Stinear. 2005. A novel mycolactone from a clinical isolate of *Mycobacterium ulcerans* provides evidence for additional toxin heterogeneity as a result of specific changes in the modular polyketide synthase. *Chem. Biochem.* **6**:1–5.
35. Johnson, P. D., T. P. Stinear, and J. A. Hayman. 1999. *Mycobacterium ulcerans*. *J. Med. Microbiol.* **48**:511–513.
36. Kaufmann, S. H. 1993. Immunity to intracellular bacteria. *Annu. Rev. Immunol.* **11**:129–163.
37. King, C. H., S. Mundayoor, J. T. Crawford, and T. M. Shinnick. 1993. Expression of contact-dependent cytolytic activity by *Mycobacterium tuberculosis* and isolation of the genomic locus that encodes the activity. *Infect. Immun.* **61**:2708–2712.
38. Krieg, R. E., W. T. Hockmeyer, and D. H. Connor. 1974. Toxin of *Mycobacterium ulcerans*. Production and effects in guinea pig skin. *Arch. Dermatol.* **110**:783–788.
39. Lagarrigue, V., F. Portaels, W. M. Meyers, and J. Aguiar. 2000. Buruli ulcer: risk of bone involvement! A propos of 33 cases observed in Benin. *Med. Trop. (Mars.)* **60**:262–266.
40. MacCallum, P., J. C. Tolhurst, G. Buckle, and H. A. Sissons. 1948. A new mycobacterial infection in man. *J. Pathol. Bacteriol.* **60**:93–122.
41. Maderna, P., and C. Godson. 2003. Phagocytosis of apoptotic cells and the resolution of inflammation. *Biochim. Biophys. Acta* **1639**:141–151.
42. Marston, B. J., M. O. Diallo, C. R. Horsburgh, Jr., I. Diomande, M. Z. Saki, J. M. Kanga, G. Patrice, H. B. Lipman, S. M. Ostroff, and R. C. Good. 1995. Emergence of Buruli ulcer disease in the Daloa region of Cote d'Ivoire. *Am. J. Trop. Med. Hyg.* **52**:219–224.
43. McDonough, K. A., and Y. Kress. 1995. Cytotoxicity for lung epithelial cells is a virulence-associated phenotype of *Mycobacterium tuberculosis*. *Infect. Immun.* **63**:4802–4811.
44. Mor, N., I. Lutsky, and L. Levy. 1981. Response in the hindfoot pad and popliteal lymph node of C57BL mice to infection with *Mycobacterium marinum*. *Isr. J. Med. Sci.* **17**:236–244.
45. Mve-Obiang, A., R. E. Lee, F. Portaels, and P. L. Small. 2003. Heterogeneity of mycolactones produced by clinical isolates of *Mycobacterium ulcerans*: implications for virulence. *Infect. Immun.* **71**:774–783.
46. Noeske, J., C. Kuaban, S. Rondini, P. Sorlin, L. Ciaffi, J. Mbuagbaw, F. Portaels, and G. Pluschke. 2004. Buruli ulcer disease in Cameroon rediscovered. *Am. J. Trop. Med. Hyg.* **70**:520–526.
47. North, R. J., and Y. J. Jung. 2004. Immunity to tuberculosis. *Annu. Rev. Immunol.* **22**:599–623.
48. Pahlevan, A. A., D. J. Wright, C. Andrews, K. M. George, P. L. Small, and B. M. Foxwell. 1999. The inhibitory action of *Mycobacterium ulcerans* soluble factor on monocyte/T cell cytokine production and NF-kappa B function. *J. Immunol.* **163**:3928–3935.
49. Palenque, E. 2000. Skin disease and nontuberculous atypical mycobacteria. *Int. J. Dermatol.* **39**:659–666.
50. Pedrosa, J., M. Florido, Z. M. Kunze, A. G. Castro, F. Portaels, J. McFadden, M. T. Silva, and R. Appelberg. 1994. Characterization of the virulence of *Mycobacterium avium* complex (MAC) isolates in mice. *Clin. Exp. Immunol.* **98**:210–216.
51. Pedrosa, J., B. M. Saunders, R. Appelberg, I. M. Orme, M. T. Silva, and A. M. Cooper. 2000. Neutrophils play a protective nonphagocytic role in systemic *Mycobacterium tuberculosis* infection of mice. *Infect. Immun.* **68**:577–583.
52. Pimsler, M., T. A. Sponsler, and W. M. Meyers. 1988. Immunosuppressive properties of the soluble toxin from *Mycobacterium ulcerans*. *J. Infect. Dis.* **157**:577–580.
53. Portaels, F., J. Aguiar, M. Debacker, A. Guedenon, C. Steunou, C. Zinsou, and W. M. Meyers. 2004. *Mycobacterium bovis* BCG vaccination as prophylaxis against *Mycobacterium ulcerans* osteomyelitis in Buruli ulcer disease. *Infect. Immun.* **72**:62–65.
54. Portaels, F., J. Aguiar, M. Debacker, C. Steunou, C. Zinsou, A. Guedenon, and W. M. Meyers. 2002. Prophylactic effect of *Mycobacterium bovis* BCG vaccination against osteomyelitis in children with *Mycobacterium ulcerans* disease (Buruli ulcer). *Clin. Diagn. Lab. Immunol.* **9**:1389–1391.
55. Prevot, G., E. Bourreau, H. Pascalis, R. Pradinaud, A. Tanghe, K. Huygen, and P. Launois. 2004. Differential production of systemic and intralésional gamma interferon and interleukin-10 in nodular and ulcerative forms of Buruli disease. *Infect. Immun.* **72**:958–965.
56. Ramakrishnan, L., and S. Falkow. 1994. *Mycobacterium marinum* persists in cultured mammalian cells in a temperature-restricted fashion. *Infect. Immun.* **62**:3222–3229.
57. Read, J. K., C. M. Heggie, W. M. Meyers, and D. H. Connor. 1974. Cytotoxic activity of *Mycobacterium ulcerans*. *Infect. Immun.* **9**:1114–1122.
58. Rosenberg, F. F., and J. Gallin. 1999. Inflammation, p. 1051–1066. *In* W. Paul (ed.), *Fundamental immunology*. Lippincott-Raven Publishers, Philadelphia, Pa.
59. Saunders, B. M., and C. Cheers. 1995. Inflammatory response following intranasal infection with *Mycobacterium avium* complex: role of T-cell subsets and gamma interferon. *Infect. Immun.* **63**:2282–2287.
60. Seiler, P., P. Aichele, B. Raupach, B. Odermatt, U. Steinhoff, and S. H. Kaufmann. 2000. Rapid neutrophil response controls fast-replicating intracellular bacteria but not slow-replicating *Mycobacterium tuberculosis*. *J. Infect. Dis.* **181**:671–680.
61. Shepard, C. C., and D. H. McRae. 1968. A method for counting acid-fast bacteria. *Int. J. Lepr. Mycobact. Dis.* **36**:78–82.
62. Silva, M. T., M. N. Silva, and R. Appelberg. 1989. Neutrophil-macrophage cooperation in the host defence against mycobacterial infections. *Microb. Pathog.* **6**:369–380.
63. Smith, P. G., W. D. Revill, E. Lukwago, and Y. P. Rykushin. 1977. The protective effect of BCG against *Mycobacterium ulcerans* disease: a controlled trial in an endemic area of Uganda. *Trans. R. Soc. Trop. Med. Hyg.* **70**:449–457.
64. Snyder, D. S., and P. L. Small. 2003. Uptake and cellular actions of mycolactone, a virulence determinant for *Mycobacterium ulcerans*. *Microb. Pathog.* **34**:91–101.
65. Stanford, J. L., W. D. Revill, W. J. Gunthorpe, and J. M. Grange. 1975. The production and preliminary investigation of Burulin, a new skin test reagent for *Mycobacterium ulcerans* infection. *J. Hyg. (London)* **74**:7–16.
66. Stienstra, Y., W. T. Van Der Graaf, G. J. te Meerman, T. H. The, L. F. de Leij, and T. S. Van Der Werf. 2001. Susceptibility to development of *Mycobacterium ulcerans* disease: review of possible risk factors. *Trop. Med. Int. Health* **6**:554–562.

67. Stinear, T., J. K. Davies, G. A. Jenkin, F. Portaels, B. C. Ross, F. Oppedisano, M. Purcell, J. A. Hayman, and P. D. Johnson. 2000. A simple PCR method for rapid genotype analysis of *Mycobacterium ulcerans*. *J. Clin. Microbiol.* **38**:1482–1487.
68. Stinear, T. P., H. Hong, W. Frigui, M. J. Pryor, R. Brosch, T. Garnier, P. F. Leadlay, and S. T. Cole. 2005. Common evolutionary origin for the unstable virulence plasmid pMUM found in geographically diverse strains of *Mycobacterium ulcerans*. *J. Bacteriol.* **187**:1668–1676.
69. Stinear, T. P., A. Mve-Obiang, P. L. Small, W. Frigui, M. J. Pryor, R. Brosch, G. A. Jenkin, P. D. Johnson, J. K. Davies, R. E. Lee, S. Adusumilli, T. Garnier, S. F. Haydock, P. F. Leadlay, and S. T. Cole. 2004. Giant plasmid-encoded polyketide synthases produce the macrolide toxin of *Mycobacterium ulcerans*. *Proc. Natl. Acad. Sci. USA* **101**:1345–1349.
70. Tanghe, A., J. Content, J. P. Van Vooren, F. Portaels, and K. Huygen. 2001. Protective efficacy of a DNA vaccine encoding antigen 85A from *Mycobacterium bovis* BCG against Buruli ulcer. *Infect. Immun.* **69**:5403–5411.
71. Tonjum, T., D. B. Welty, E. Jantzen, and P. L. Small. 1998. Differentiation of *Mycobacterium ulcerans*, *M. marinum*, and *M. haemophilum*: mapping of their relationships to *M. tuberculosis* by fatty acid profile analysis, DNA-DNA hybridization, and 16S rRNA gene sequence analysis. *J. Clin. Microbiol.* **36**:918–925.
72. Travis, W. D., L. B. Travis, G. D. Roberts, D. W. Su, and L. W. Weiland. 1985. The histopathologic spectrum in *Mycobacterium marinum* infection. *Arch. Pathol. Lab Med.* **109**:1109–1113.
73. Uganda Buruli Group. 1969. BCG vaccination against *Mycobacterium ulcerans* infection (Buruli ulcer). First results of a trial in Uganda. *Lancet* **293**:111–115.
74. Van Der Werf, T. S., W. T. Van Der Graaf, J. W. Tappero, and K. Asiedu. 1999. *Mycobacterium ulcerans* infection. *Lancet* **354**:1013–1018.
75. Walsh, D. S., W. M. Meyers, R. E. Krieg, and G. P. Walsh. 1999. Transmission of *Mycobacterium ulcerans* to the nine-banded armadillo. *Am. J. Trop. Med. Hyg.* **61**:694–697.
76. Westenbrink, B. D., Y. Stienstra, M. G. Huitema, W. A. Thompson, E. O. Klutse, E. O. Ampadu, H. M. Boezen, P. C. Limburg, and T. S. van der Werf. 2005. Cytokine responses to stimulation of whole blood from patients with Buruli ulcer disease in Ghana. *Clin. Diagn. Lab. Immunol.* **12**:125–129.
77. Wyllie, A. H., J. F. Kerr, and A. R. Currie. 1980. Cell death: the significance of apoptosis. *Int. Rev. Cytol.* **68**:251–306.

---

Editor: J. L. Flynn